 FDMP, vol.13, no.3, pp.189-212, 2017

Mixed Convection of Nanofluids inside a Lid-Driven Cavity Heated by a Central Square Heat Source

Fatima-zohra Bensouici[1, *] and Saadoun Boudebous[2]

Abstract: A numerical work has been performed to analyze the laminar mixed convection of nanofluids confined in a lid driven square enclosure with a central square and isotherm heat source. All the walls are cooled at constant temperature, and the top wall slides rightward at constant velocity. The simulations considered four types of nanofluids (Cu, Ag, Al_2O_3 and TiO_2)-Water. The governing equations were solved using finite volume approach by the SIMPLER algorithm. Comparisons with previously published work are performed and found to be in good agreement. The influence of pertinent parameters such as Richardson number, size of the heat source, solid volume fraction and type of nanofluid, on the heat transfer characteristics of mixed convection is studied. For all the simulations, the Reynolds number is fixed to Re=100. The results show that a better cooling of the heat source is obtained at a size of S=0.25 for copper-water nanofluid at Ri=100 where the buoyancy is stronger. As a consequence, we can economise the lid driven energy. The results also show that adding nanoparticles into pure water improves heat transfer in the enclosure. Furthermore, Copper and Silver-water nanofluids yield the best heat transfer enhancement in comparison with the other nanofluids.

Keywords: Mixed convection, nanofluid, lid-driven cavity, heat source, numerical simulation, heat transfer enhancement.

Nomenclature

C_p	specific heat [$J \cdot kg^{-1} \cdot K^{-1}$]
g	gravitational acceleration [$m \cdot s^{-2}$]
Gr	Grashof number
k	thermal conductivity [$W \cdot m^{-1} \cdot K^{-1}$]
l	size of the heat source [m]
L	size of the cavity [m]
Num	mean Nusselt number of the heat Source, $Num = \frac{-k_{nf}}{k_f} \int_A \frac{\partial \theta}{\partial X} dY$

[1]Faculté de Génie des Procédés Pharmaceutiques, Université de Constantine 3, UVN05, Ali Mendjeli Nouvelle Ville, Khroub, Constantine 25000
[2]Département de Mécanique, Université Larbi BenM'hidi, Oum el Bouaghi ALGERIE
[*]Corresponding Author : Fatima-zohra Bensouici. Email: fzbensouici9@gmail.com.

Num1	mean Nusselt number of the left face of the heat source
Num2	mean Nusselt number of the top face of the heat source
Num3	mean Nusselt number of the right face of the heat source
Num4	mean Nusselt number of the bottom face of the heat source
Num, w	mean Nusselt number of the heat source for pure water
P	pressure [Pa]
Pr	Prandtl number ($= \nu_f/\alpha_f$)
Re	Reynolds number (= $U_0 L/\nu_f$)
Ri	Richardson number ($= Gr/Re^2$)
S	dimensionless heat source size (S = l/L)
T	temperature [K]
u, v	velocity components in x, y directions [$m \cdot s^{-1}$]
U, V	dimensionless velocity components
x, y	cartesian coordinates [m]
U_0	lid velocity [$m \cdot s^{-1}$]
X, Y	dimensionless coordinates.

Greek symbols

α	thermal diffusivity [$m^2 \cdot s^{-1}$]
φ	nanoparticles volume fraction
μ	dynamic viscosity [$kg \cdot m^{-1} \cdot s^{-1}$]
β	thermal expansion coefficient [K^{-1}]
Θ	dimensionless temperature (= $(T-T_c)/(T_h-T_c)$)
ν	kinematic viscosity [$m^2 \cdot s^{-1}$]
ρ	density [$kg \cdot m^{-3}$]
ψ	stream function

Subscripts

h	hot
c	cold
f	fluid
nf	nanofluid
max	maximal
w	wall

1 Introduction

Convection heat transfer in enclosures has many applications such as cooling of electronic devices, nuclear reactors, solar collectors, heating and cooling of buildings, glass-making

industry, but low thermal conductivity of conventional heat transfer fluids such as water and oils is a main limitation in enhancing heat transfer. To overcome this impediment, researchers developed fluids with advanced heat transfer properties: nanofluids which are suspensions of small particles in a base pure fluid.

In the recent years, numerous studies on the enhancement of convective heat transfer by using nanofluids were performed: Elif Büyük ögüt [Elif Büyük ögüt (2009)] numerically investigated natural convection heat transfer of nanofluids in an inclined square enclosure, the results show that the average transfer rate increases significantly as Rayleigh number and particle volume fraction increase, and decrease according to the ordering Ag, Cu, CuO, Al_2O_3, and TiO_2. Ghasemi et al. [Ghasemi and Aminossadati (2009)] performed a numerical study of natural convection in a differentially heated inclined enclosure filled with water-CuO nanofluid. They found an optimum solid volume fraction which maximizes the heat transfer rate. Garoosi et al. [Garoosi, Bagheri and Talebi (2013)] studied numerically buoyancy driven convection in a cavity filled with nanofluids, with several pairs of heaters and coolers inside. They investigated the effects of the design parameters, volume fraction and types of nanoparticles. Their results showed that the highest and the lowest impacts of design parameters, on the enhancement of heat transfer rate are caused by changing the HAC's position and types of nanoparticles respectively. Moreover, they found that heat transfer increases with changing orientation of HAC from horizontal to vertical for the entire range of Rayleigh's number. Their simulations indicated that heat transfer can be enhanced more efficiently by increasing the number of HAC than increasing the HAC's size. The optimum value of volume fraction is found to be equal to 1% and beyond that the heat transfer decreases. Wang et al. [Wang, Meng, Zeng et al. (2014)] carried out a numerical study of natural convective heat transfer of copper-water nanofluid in a square cavity with time-periodic boundary temperature. The results illustrate that the heat transfer rate increases using copper nanoparticles. Sivasankaran et al. [Sivasankaran and Pan (2014)] investigated numerically the effects of nanofluid, amplitude ratio and phase deviation of sinusoidal temperature distribution, on natural convection flow in a square enclosure They observed that the heat transfer rate can essentially be enhanced by non-uniform heating of both walls as compared to the case of uniform heating on one wall. The heat transfer rate is increased when increasing the amplitude ratio between the sinusoidal temperature variations on the walls and the volume fraction of nanoparticles. Also, the heat transfer rate increases when increasing the Rayleigh number. Abu-Nada et al. [Abu-Nada and Oztop (2011)] reported a numerical study, on heat transfer enhancement of Al_2O_3-water nanofluids in natural convection applied to differentially heated wavy cavities. They observed that the addition of a nanoparticle of Al_2O_3 into the base fluid increases the mean Nusselt number. Rashidi et al. [Rashidi, Mahian, Lorenzini et al. (2014)] investigated natural convection in a square cavity filled with water-Al_2O_3 nanofluid under non-uniform heat flux on the bottom wall. The optimal profile of heat flux is determined where Nusselt number is maximized.

Forced convection is one of the most important subjects in many technological applications like high performance boilers, chemical catalytic reactors, power plants. Management of heat transfer for its enhancement or reduction in these systems is an

essential task from an energy saving perspective. Heidary et al. [Heidary and Kerman (2012)] carried out a numerical study of nanofluid heat transfer and fluid flow in a channel with blocks attached to the bottom wall. Simulations showed that heat transfer in channels can enhance up to 60% due to the presence of nanoparticles and the usage of blocks on hot walls. Abdellahoum et al. [Abdellahoum, Mataoui and Oztop (2015)] presented a numerical investigation of forced convection of nanofluid over a heated cavity in a horizontal duct. They found that the average Nusselt number increases with the volume fraction of nanoparticles for the whole tested range of Reynolds number.

Mixed convection flow occurs in lid-driven cavities due to both shear force generated by the movement of the lid wall and the buoyancy force created by thermal heating in the cavity. Abu-Nada et al. [Abu-Nada and Chamkha (2010)] detailed a numerical simulation of laminar mixed convection flow in a lid-driven inclined square enclosure filled with water-Al_2O_3 nanofluid. They found that significant heat transfer enhancement can be obtained due to the presence of nanoparticles. Many other researchers presented works on mixed convection. Kalteh et al. [Kalteh Javaherdeh and Azarbarzin (2014)] numerically studied the effects of nanofluid properties, on laminar mixed convection of a triangular heat source and concluded that suspending the nanoparticles in pure fluid leads to a significant heat transfer enhancement, also increasing the nanoparticles diameter leads to a decrease in the average Nusselt number for all Richardson numbers. Rahman et al. [Rahman, Billah, Hasanuzzaman et al. (2012)] numerically studied the effects of Reynolds and Prandtl numbers on mixed convective flow and heat transfer characteristics inside a ventilated cavity in presence of a heat-generating solid circular obstacle placed at the center. Their findings indicate that the flow and thermal fields as well as the heat transfer rate, the Drag force and the average fluid temperature in the cavity depend significantly on these parameters. Roslan et al. [Roslan, Saleh and Hashim (2012)] studied convective heat transfer in a differentially heated square enclosure with an inner rotating cylinder, the free space between the cylinder and the enclosure walls is filled with water (Cu, Ag, Al_2O_3 and TiO_2) nanofluids. They observed that the strength of the flow circulation is much stronger for a higher nanoparticle concentration, a better thermal conductivity value and a smaller cylinder. Akand et al. [Akand, Sharif and Carlson (2012)] performed a numerical study, using ANSYS FLUENT, on laminar mixed convection in a square cavity and with an isothermally heated square blockage inside at Pr=0.71. Their results show that for any size of the blockage placed anywhere in the cavity, the average Nusselt number does not change significantly with increasing Richardson number until it approaches the value of the order of 1 beyond which the average Nusselt number increases rapidly with the Richardson number. They found that the best heat transfer is obtained when the blockage is placed around the top left and bottom right corners of the cavity. Khandakar et al. [Khandakar, Sharif and Akand (2015)] investigated numerically, the laminar mixed convection in a lid driven square cavity with two isothermally heated square internal blockages at Pr=0.71. They developed correlations between average Nusselt, Richardson and Reynolds numbers and observed that the average Nusselt number on the blockages surfaces increases with increasing Reynolds and Richardson numbers, and changes significantly with change of the placement of the blockages and the distance between them. Selimefendigil et al. [Selimefendigil and Öztop (2014)] have performed using COMSOL, a numerical study,

of mixed convection nanofluid lid driven square enclosure with a central rotating cylinder, the bottom wall is the only heated surface. It is observed that 17% of heat transfer enhancement is obtained for Ri=10 when compared to flow at Ri=1. Averaged heat transfer decreases with increasing Hartmann number and the rotation of cylinder enhances heat transfer. Also, when the solid volume fraction of nanoparticle is increased, heat transfer increases. Rashmi et al. [Rashmi, Khalid, Ismail et al. (2015)] experimentally and numerically investigated the heat transfer enhancement using carbon nanotube nanofluids as a cooling fluid in a concentric tube laminar flow heat exchanger. They measured conductivity, density and rheology of the nanofluid as function of temperature. The results showed thermal conductivity enhancement from 4% to 125% and nearly 70% enhancement in heat transfer with increase in flow rate. Moradi et al. [Moradi, Bazooyar, Seyed et al. (2015)] studied experimentally natural convection heat transfer of Al_2O_3 and TiO_2/water nanofluids in a cylindrical enclosure. Results show that adding nanoparticles to water has a negligible or even adverse influence upon natural convection heat transfer of water especially for high values of the Rayleigh number.

The aim of the present work is to study numerically mixed convection in a lid-driven square enclosure with a central square and isotherm heat source. The respective effects of varying the Richardson number, the size of the heat source, solid volume fraction and the type of nanofluids, on the fluid flow and heat transfer have been investigated and discussed.

2 Mathematical formulation

2.1 Problem description

The physical system considered in the present study is shown in Fig. 1. A Cartesian co-ordinate system is used with origin at the left corner of the domain. We investigate mixed convection in a lid-driven square enclosure with sides of length L, and a central heat generating square solid. This heat source has uniform temperature T_h and its dimensionless size is S. All the walls are cooled at uniform temperature T_c and the top wall slides rightward at constant speed U_0. Under all conditions $\Delta T=T_h-T_c$ is less than 8°c.The fluid in the cavity is a water based nanofluid, Newtonian, incompressible and the flow is conceived as two-dimensional and laminar. The nanoparticles are assumed to have uniform shape and size. It is considered that thermal equilibrium exists between the base fluid and nanoparticles and no slip exists between the two media. The thermo-physical properties of the nanofluid are considered to be constant except the density variation in the body forces term of momentum equation which is satisfied by the Boussinesq's approximation. The gravitational acceleration acts in the negative *y* direction. All solid boundaries are assumed to be rigid and there are not slip walls. The thermophysical properties of the fluid and solid phases are shown in Tab. 1.

Table 1: Thermophysical properties of base fluid and nanoparticles at 298°k [Moumni, Welhezi, Djebali et al. (2015)] and [Chemloul and Belmiloud (2016)]

Property	**Water**	**Cu**	**Ag**	**TiO_2**	**Al_20_3**
C_p (J/kg K)	4179	385	235	686.2	765
ρ (kg/m^3)	997.1	8933	10500	4250	3970
K (W/m K)	0.613	401	429	8.9538	40
β 10^5 (1/K)	21	1.67	1.89	0.9	0.85

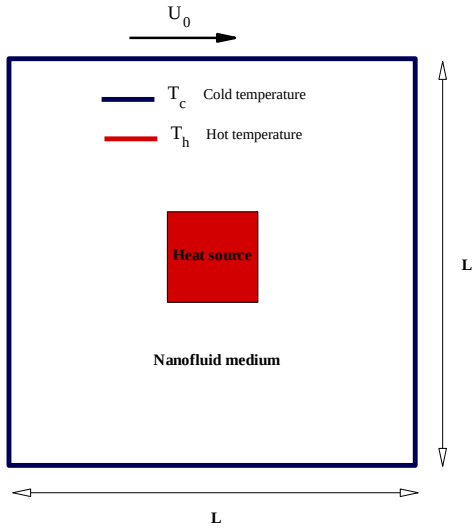

Figure 1: Schematic diagram of physical model

2.2 Governing equations

The flow is modeled by the Navier-Stokes equations. The conservation equations of mass, momentum, and energy for a steady-state, two-dimensional laminar mixed convection and incompressible flow are expressed in dimensional form as follows.

Continuity

$$\frac{\partial u}{\partial x}+\frac{\partial v}{\partial y}=0 \tag{1}$$

X-momentum

$$u\frac{\partial u}{\partial x}+v\frac{\partial u}{\partial y}=-\frac{1}{\rho_{nf}}\frac{\partial p}{\partial x}+\nu_{nf}\left\{\frac{\partial^2 u}{\partial x^2}+\frac{\partial^2 u}{\partial y^2}\right\} \tag{2}$$

Y-momentum

$$u\frac{\partial v}{\partial x}+v\frac{\partial v}{\partial y}=-\frac{1}{\rho_{nf}}\frac{\partial p}{\partial y}+\nu_{nf}\left\{\frac{\partial^2 v}{\partial x^2}+\frac{\partial^2 v}{\partial y^2}\right\}+\frac{(\rho\beta)_{nf}}{\rho_{nf}}g(T-T_C)$$

(3) *Energy*

$$u\frac{\partial T}{\partial x}+v\frac{\partial T}{\partial y}=\alpha_{nf}\left\{\frac{\partial^2 T}{\partial x^2}+\frac{\partial^2 T}{\partial y^2}\right\}) \tag{4}$$

Thermal diffusivity and effective density of the nanofluid are:

$$\alpha_{nf} = \frac{k_{nf}}{(\rho c_p)_{nf}} \tag{5}$$

$$\rho_{nf} = \varphi\rho_s + (1-\varphi)\rho_f \tag{6}$$

Thermal expansion coefficient and heat capacity of the nanofluid are:

$$(\rho\beta)_{nf} = \varphi(\rho\beta)_s + (1-\varphi)(\rho\beta)_f \tag{7}$$

$$(\rho c_p)_{nf} = \varphi(\rho c_p)_s + (1-\varphi)(\rho c_p)_f \tag{8}$$

The effective viscosity of the nanofluid was proposed by
Brinkman [Brinkman (1952)] as follows:

$$\mu_{nf} = \frac{\mu_f}{(1-\varphi)^{2.5}} \tag{9}$$

The effective thermal conductivity of the nanofluid is calculated by the Maxwell model:

$$\frac{k_{nf}}{k_f} = \frac{k_s+2k_f-2\varphi(k_f-k_s)}{k_s+2k_f+\varphi(k_f-k_s)} \tag{10}$$

The dimensionless parameters may be presented as:

$$X = \frac{x}{L}\ Y = \frac{y}{L}\ U = \frac{u}{U_0},\ V = \frac{v}{U_0},\ \Theta = \frac{T-T_c}{T_h-T_c}\ P = \frac{(p+\rho gy)L^2}{\rho_{nf}\ U_0^2} \tag{11}$$

The dimensionless forms of the above governing equations become as follows:

Continuity

$$\frac{\partial U}{\partial X} + \frac{\partial V}{\partial Y} = 0 \tag{12}$$

X-momentum

$$U\frac{\partial U}{\partial X} + V\frac{\partial U}{\partial Y} = -\frac{\partial P}{\partial X} + \frac{1}{Re}\frac{\rho_f}{\rho_{nf}}\frac{1}{(1-\varphi)^{2.5}}\left\{\frac{\partial^2 U}{\partial X^2} + \frac{\partial^2 U}{\partial Y^2}\right\} \tag{13}$$

Y-momentum

$$U\frac{\partial V}{\partial X} + V\frac{\partial V}{\partial Y} = -\frac{\partial P}{\partial Y} + \frac{1}{Re}\frac{\rho_f}{\rho_{nf}}\frac{1}{(1-\varphi)^{2.5}}\left\{\frac{\partial^2 V}{\partial X^2} + \frac{\partial^2 V}{\partial Y^2}\right\} + \frac{(\rho\beta)_{nf}}{\rho_{nf}\beta_f}Ri\Theta \tag{14}$$

Energy equation

$$U\frac{\partial \Theta}{\partial X} + V\frac{\partial \Theta}{\partial Y} = \frac{\alpha_{nf}}{\alpha_f}\frac{1}{Re\ Pr}\left\{\frac{\partial^2 \Theta}{\partial X^2} + \frac{\partial^2 \Theta}{\partial Y^2}\right\} \tag{15}$$

Where U and V are dimensionless velocity components in the X and Y directions, respectively. The non-dimensional parameters that appear in the above equations are the Reynolds number $Re = U_0 L/\nu_f$ Prandtl number $Pr = \nu_f/\alpha_f$, Richardson number $Ri = Gr/Re^2$, Grashof number $Gr = g\beta_f \Delta T L^3/\nu_f^2$ and solid volume fraction of the nanoparticles φ.

2.3 Boundary conditions

At X=0 and $0 \le Y \le L$, U=0, V= 0, Θ_c=0

At X=L and $0 \le Y \le L$, U=0, V= 0, Θ_c=0

At Y=L and $0 \le X \le L$, U=U_0 = 1, V=0, Θ_c=0 (16)

At Y=0 and $0 \le X \le L$, U=0, V=0, Θ_c=0

At the heat source surfaces: U=0, V=0, Θ_h=1

3 Numerical method and code validation

The governing Eq. (12-15) with corresponding boundary conditions Eq. (16) was solved using the finite volume method [Patankar (1980)]. Scalar quantities (P and Θ) are stored at the center of these volumes, whereas the vectorial quantities (u and w) are stored on the faces. The governing equations were discretized using the power-law scheme. The SIMPLER algorithm was used to determine the pressure from continuity equation. The discretized algebraic equations are solved by the line-by-line tri-diagonal matrix algorithm (TDMA). Convergence was obtained when the maximum relative change between two consecutive iteration levels fell below 10^{-4}, for U, V and Θ. Calculations were carried out on a PC with a 3.2 GHz CPU.

3.1 Grid independence study

In order to find the proper grid size which yields reasonably accurate predictions, grid sensitivity tests are conducted. Three uniform grid meshes are used 50×50, 80×80 and 100×100 nodes for Re=100, $Ri=Gr/Re^2=0.1$, $\varphi=0.04$, S=0.25 and the results of the grid variation study are presented in Tab. 2. Based on the results, of which the 80×80 grid is adopted for all computations.

Table 2: Mean Nusselt number of the heat source obtained for each grid size, $\varphi=0.04$, Re=100, Ri=0.1

Mesh size	Num
50×50 nodes	5.106859
80×80 nodes	4.824586
100×100 nodes	4.786532

3.2 Code validation

In order to verify the accuracy of the present study, the numerical code was validated with the numerical results of Rahman et al. [Rahman, Billah, Hasanuzzaman et al. (2012)] and Muthtamilselvan et al. [Muthtamilselvan, Kandaswamy and Lee (2010)]. For Rahman et al. [Rahman, Billah, Hasanuzzaman et al. (2012)], a comparison of mean Nusselt number (at the hot wall) for mixed convection in a lid-driven square enclosure was presented. The two horizontal walls of the enclosure are insulated, while the vertical walls are kept differentially heated by constant temperature. For Muthtamilselvan et al. [Muthtamilselvan, Kandaswamy and Lee (2010)], we compared also mean Nusselt number at the hot wall for mixed convection in a lid-driven enclosure filled with nanofluids. The cavity is heated at the top wall and cooled at the bottom one, while the vertical boundaries are insulated. The results are respectively documented in Tab. 3 and Tab. 4. The comparisons reveal an excellent agreement with the reported studies.

Table 3: Comparison of mean Nusselt number obtained in our results with those of Rahman et al. [Rahman, Billah, Hasanuzzaman et al. (2012)]

	Num		
Ri	**Rahman**	**Present study**	**% difference**
0.0	4.50	4.662	3.60
1.0	3.80	3.995	5.13
3.0	4.65	4.868	4.69
5.0	5.10	5.215	2.25

Table 4: Comparison of mean Nusselt number obtained in our results with those of Muthtamilselvan et al. [Muthtamilselvan, Kandaswamy and Lee (2010)]

	Num		
φ	**Muthtamilselvan**	**Present study**	**% difference**
0.00	2.26	2.282	0.97
0.02	2.40	2.416	0.67
0.04	2.56	2.558	0.08
0.06	2.73	2.707	0.84
0.08	2.91	2.866	1.51

4 Results and discussion

Numerical analysis has been performed at the following values of governing parameters: Reynolds number Re=100, Richardson number (Ri=0.01, 1, 10, 100), dimensionless sizes of the heat source (S=0.25, 0.50, 0.75), solid volume fraction (φ=0, 0.02, 0.04, 0.06). We considered four types of Nanofluids.

4.1 Effect of the Richardson number

In order to study the mixed convection in the square cavity filled with nanofluids and containing the heated source, the Richardson number «$Ri=Gr/Re^2$» represents a key factor, which characterizes the relative importance of buoyancy driven natural convection to the lid driven forced convection. Simulations were accomplished for the Richardson numbers (Ri= 0.01, 1, 10 and 100) to see its effect on the flow structure and heat transfer in the cavity. The other parameters kept constant in this section are: Reynolds number Re=100, the nanofluid chosen for this effect is Copper-water, its volume fraction is φ=0.04 and the heat source size is S=0.25.

Fig. 2 draws the variation of the mean Nusselt number at the heat source surface versus the Richardson number. We observe that for Ri<1, the mean Nusselt number remains constant until Ri reaches the value of 1. Then by increasing Richardson number Ri>1 (i.e. passing from the forced convection dominating towards the natural convection

dominating effect), the mean Nusselt number increases by 175.61% at Ri=100. As a result of this significant improvement in heat transfer inside the cavity, we can produce a better cooling of the heat source by increasing the Richardson number to natural convection dominating regime. This will allow us to reduce the velocity of the lid and economize the energy required for its movement.

In order to examine the effect of the Richardson number on the heat removal rate from heat source faces, we investigated the variation of the mean Nusselt numbers of the heat source faces Num1, Num2, Num3, and Num4 with the Ri varying from 0.01 to 100, the results are presented in Tab. 5. We remark that the mean Nusselt number Num3 of the right face is better than the other faces for Ri<10, but for Ri=100, the Nusselt number Num1 of the left face becomes higher than the other's.

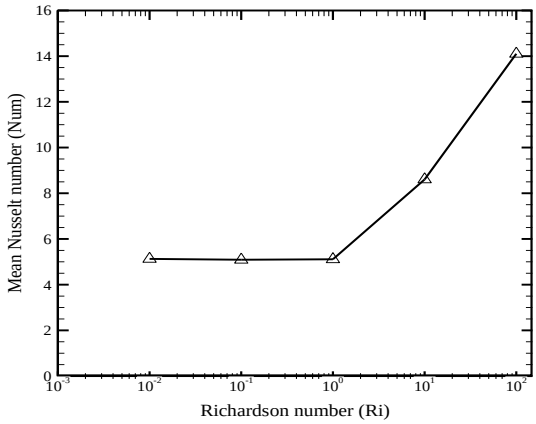

Figure 2: Variation of the mean Nusselt number at the heat source surface with the Richardson numbers (Ri=0.01, 1, 10, 100), for copper-water nanofluid, S=0.25, Re=100 and φ=0.04

Table 5: Variation of the mean Nusselt numbers Num1, Num2, Num3, and Num 4 at the faces of the heat source with the Richardson numbers, for cavity filled with copper-water nanofluid, φ =0.04, Re=100 and S=0.25

Ri/ Nu faces	**Num1**	**Num2**	**Num3**	**Num4**
Ri=0.01	0.893	1.201	1.856	1.176
Ri=1	1.224	0.994	1.582	1.317
Ri=10	2.436	1.196	2.581	2.391
Ri=100	4.322	1.955	4.234	3.592

Fig. 3 illustrates the effect of different Richardson numbers (Ri=0.01, 1, 10,100) on the streamline and isotherm contours. For small values of Richardson number (Ri=0.01), the flow and temperature fields within the cavity are dominated by forced convection effect: the flow is characterized by a strong rotating clockwise cell with its center near the top right corner of the enclosure, this vortex is generated by the rightward motion of the upper lid dragging the adjacent fluid. By increasing Richardson number to moderate

values (Ri=1.0), buoyancy and shear forces are equally important, we can see the appearance of a minor eddy near the left bottom in addition to the previous main cell. For another increase of Richardson number to large values (Ri=10), where the flow and temperature fields are dominated by natural convection effect, we observe that the natural upward flow in the left and right regions of the cavity become more important and we obtain two vertical recirculation cells, a clockwise circulating cell on the right and counter clockwise circulating one on the left. For Ri=100, we observe that the two cells become of similar importance and the fluid rises around the heat source as a thermal plume, due to the buoyancy driven natural convection. An increase in Ri leads to an intensification of the convective flow which can be demonstrated by comparison of the magnitude of maximum stream functions at different Richardson numbers.

$\psi_{max}^{Ri=0.01}$=0.000002757< $\psi_{max}^{Ri=1}$=0.000029103< $\psi_{max}^{Ri=10}$=0.1395433< $\psi_{max}^{Ri=100}$=0.7698158.

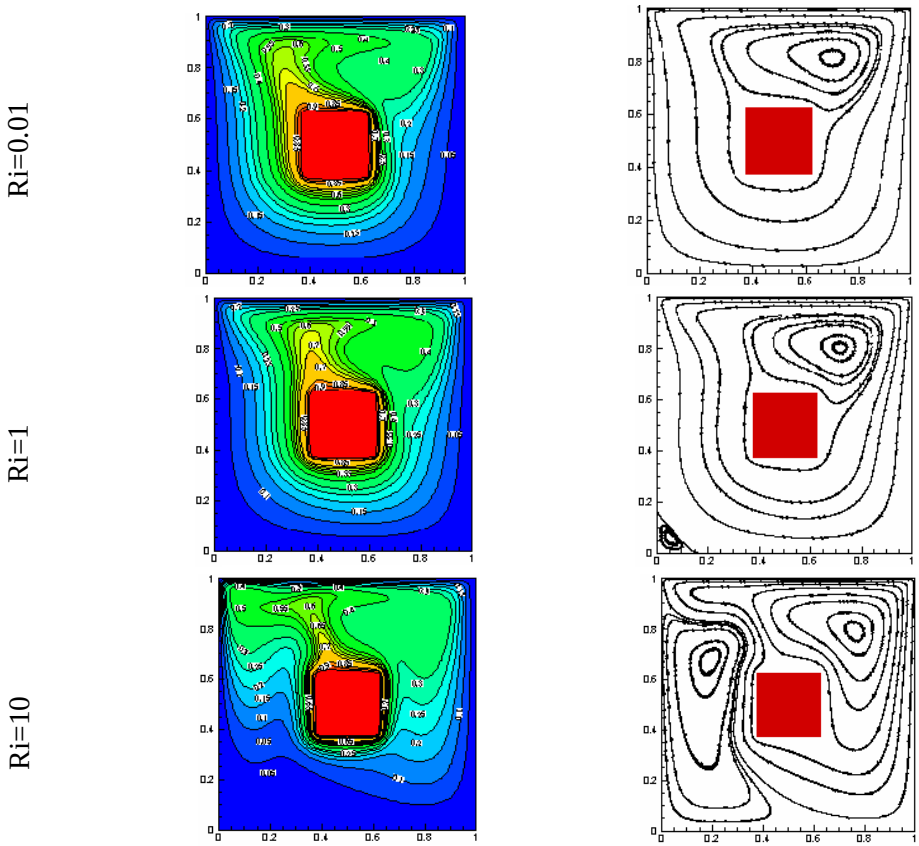

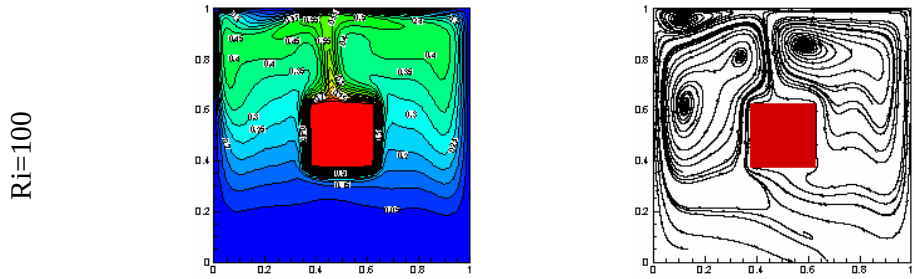

Figure 3: Isotherms (a) and streamlines (b) for copper-water filled cavity at different Richardson numbers (Ri=0.01, 1, 10, 100), for Re=100, S=0.25 and φ=0.04.

As the Richardson number is increased, the temperature fields are changed and the isotherms get compacted near the top of the cavity and around the corners of the heat source, which indicates the development of thin boundary layers with large temperature gradients, and high heat flux from these surfaces.

Fig. 4 (a) presents the v-velocity profiles along the horizontal mid-plane (Y=0.5) of the enclosure for various values of the Richardson number Ri (Ri=0.01, 1, and 10). The space around the heat source is divided into two vertical channels. The left channel is between the left cavity wall and the left surface of the heat source and the right channel is between the right cavity wall and the right side of the heat source. When we observe the v-velocity profiles, we see that for the values of Ri≤1, the flow is downward in the right channel and upward in the left one. Also, at high values of Richardson number (Ri=10), the flow is ascendant near the vertical sides of the heat source and descendant next to the lateral sides of the enclosure, the presence of the two strong vertical cells is apparent.

Fig. 4 (b) illustrates the u-velocity profiles along the vertical mid-plane(X=0.5) of the cavity, for different Richardson numbers Ri (Ri=0.01, 1, and 10), we observe that the velocity starts with positive values in the space between the cavity lid and the top surface of the heat source, takes negative values and becomes zero at the heat source surface which confirm the presence of the recirculation cell on the top of the heat source. In the lower space of the cavity, the velocity exhibits negative parabolic flow especially for Ri ≤1. These profiles are conformed to the specified boundary conditions and the flow pattern in Fig. 3.

4.2 Effect of the heat source size

In this section, we will investigate the influence of increasing the heat source size S, on heat transfer and fluid flow. Different source sizes (S=0.25, 0.5, and 0.75) are considered in this configuration. The cavity is filled with Copper-water nanofluid. The parameters kept constant in this section are: Re=100 and the solid volume fraction φ =0.04. Simulations were accomplished for the Richardson numbers (Ri=0.01, 1, 10 and 100).

The Fig. 5 shows the variation of the mean Nusselt number in function of the heat source size and Richardson number.

We remark that for heat source sizes (S=0.25 and 0.5), the mean Nusselt number doesn't

vary so much for (Ri<1), but beyond the value of Ri=1, the mean Nusselt number increases more rapidely. However, for S=0.75, the mean Nusselt number remains constant until Ri=10, then increases by increasing the Richardson number.

For Ri≤1, when increasing the heat source size from S=0.25 to S=0.5, the mean Nusselt number decreases from 5.12 to about 4.55, however when we increase the size from S=0.50 to S=0.75, the mean Nusselt number increases to about 5.99. For the natural convection dominating regime (Ri=10), when increasing the heat source size from S=0.25 to S=0.5, the mean Nusselt number decreases from about 8.60 to about 5.80, but when we increase this size to S=0.75, the mean Nusselt number increases to about 6.

For higher values of Richardson number (Ri=100), when we increase the heat source size from S=0.25 to S=0.5, the mean Nu number decreases from about 14.10 to 9.97 then it doesn't change when S increases to S=0.75. We conclude that at a fixed Ri number, the mean Nusselt number decreases when the heat source size is increased from S=0.25 to S=0.50, then increases for a further increase of the heat source size. For S=0.75, the mean Nusselt number remains constant until Ri reaches Ri=10, but has higher values in comparison with the other heat source sizes.

The highest Nusselt number is obtained for the lower heat source size studied S=0.25 at Ri=100.

Fig. 6 illustrate streamline and isotherm contours at various Richardson numbers (Ri= 0.01, 1, 10) and for the following sizes of the heat source (S=0.5, and 0.75). Compared with Fig. 3, at low values of Richardson number (Ri=0.01), we observe in the streamline contours, when increasing the heat source size from S=0.25 to S=0.50, that the main recirculation bubble on the top of the enclosure is compacted between the lid and the top of the heat source and the flow becomes like a channel flow in the other parts of the cavity. By increasing more the size of the heat source to S=0.75, this cell is more and more compressed while the flow is still like a channel flow in all the remaining parts of the cavity.

The same observations are done when increasing Richardson number to (Ri=1), where mixed convection is the dominating effect, the only differences are the appearance of a minor eddy in the left bottom of the enclosure which becomes more little for S=0.50 and disappears for S=0.75. With another increase of Richardson number to (Ri=10), the upward flows become very important due to buoyancy driven natural convection, we can observe two vertical cells of different sizes and at their contact surface, on the left top of the heat source, the fluid rises like a plume and low temperatures are observed in the bottom part of the enclosure. These observations are done for both cases of S=0.25 and S=0.50, the difference between them is that for S=0.50, the vertical cells observed have distant cores: one is near the left side and the other is near the top right side. For S=0.75, the vertical cells are squeezed in their respective vertical channels.

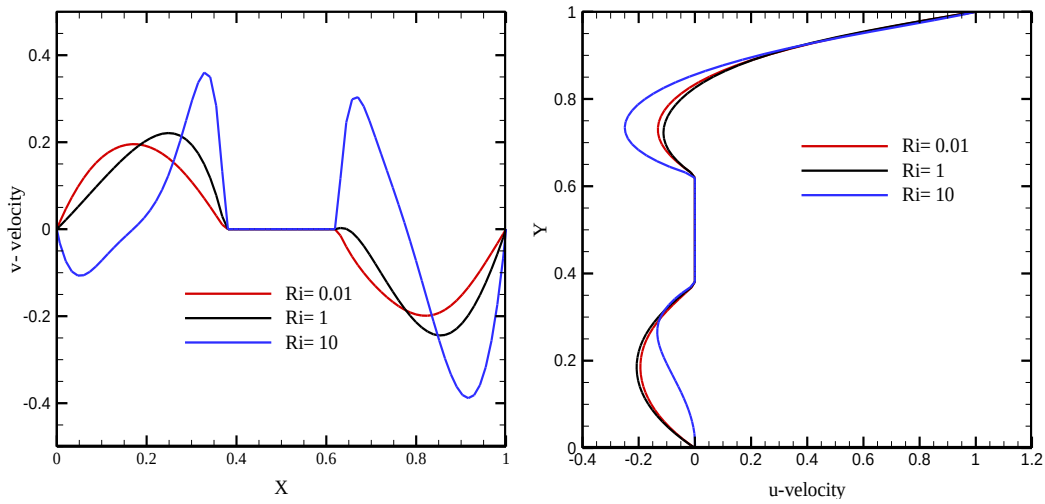

(a) (b)

Figure 4: (a) v-velocity and (b) u-velocity profiles along the horizontal and vertical mid-planes respectively in the copper-water filled cavity at different Richardson numbers (Ri =0.01, 1, 10), for Re=100, S=0.25 and φ=0.04

For all regimes, as the heat source size is increased, temperature distributions are changed.

Fig. 7 (a) presents the hydrodynamic behaviour of the convective flows in terms of the v-velocity profiles along the horizontal mid-plane(Y=0.5) of the enclosure for various values of the heat source size (S=0.25, 0.5 and 0.75) and at the Richardson numbers Ri (Ri= 0.01, 1, and 10). When we observe these profiles, we see that for all the sizes of the heat source, at values of Ri≤1, the flow is downward in the right channel and upward in the left one. At Ri=10, for S=0.25 and S=0.50, the presence of strong and vertical recirculation cells is evident. Concerning the case of S=0.75, these cells are compressed in their respective channels and the v-velocity exhibits parabolic profiles. The u-velocity profiles illustrated in Fig. 7 (b) are parabolic in all cases and all regimes. We observe that the intensity of the vertical and horizontal components of velocity is larger for high values of Richardson number.

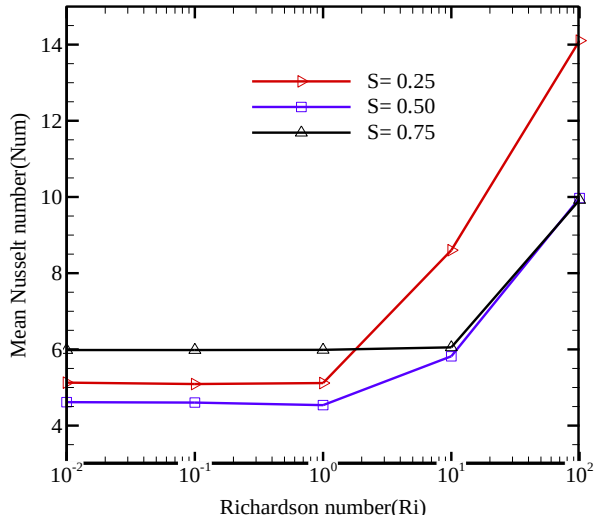

Figure 5: Variation of mean Nusselt number with Richardson number (Ri=0.01, 0.1, 1, 100), for different heat source sizes (S=0.25, 0.50, 0.75), Re=100 and φ=0.04

4.3 Effect of the solid volume fraction

To study the effect of solid volume fraction, on the flow and heat transfer, in the cavity filled with the copper-water nanofluid and subjected to a heat source with a size taken as S=0.25. Computations were carried out for φ taking the values 0, 0.04 and 0.06 and for Richardson numbers (Ri=0.01, 1, 10). The parameter kept constant in this section is Reynolds number Re=100.

Fig. 8 displays the effect of the nanoparticles volume fraction, on the mean Nusselt number of the heat source surface at different Richardson numbers, we can see that increasing the solid volume fraction of the nanofluid leads to an increase of the mean Nusselt number for all studied regimes, we note that more intensive increase of mean Nusselt number occurs at low Ri.

Fig. 9 and 10 illustrate streamline and isotherm contours at various Richardson numbers (Ri=1, 10) respectively and for different values of copper volume fractions. Clear differences are observed in the isotherm contour plots of Cu-water nanofluid compared to the case of pure water (φ=0), we observe that increase in solid volume fraction leads to decrease of the fluid temperature in the enclosure. However, increasing the solid volume fraction of nanoparticles does not influence the intensity of the stream function for all the Richardson numbers studied. This can clearly be proved by comparison of the magnitude of maximum stream functions obtained for different solid volume fraction of Cu-water nanofluid in Tab. 6.

Fig. 11 (a) and Fig. 11 (b) present respectively the v-velocity profiles along the horizontal mid-plane (Y=0.5) and u-velocity profiles along the vertical mid-plane (X=0.5) of the enclosure at different Richardson numbers (Ri=0.01, 1, 10), for pure water and the following values of copper volume fraction φ=0.04 and 0.06. Increasing the solid volume fraction does not influence so much the velocity profiles for Ri≤10.

4.4 Effect of the nanofluid material

We examine in this section the effects of nano-suspensions material, on the heat transfer rate, for the four types of nanoparticles: Cu, Ag, Al_2O_3 and TiO_2. The enclosure is subjected to a central heat source with a size taken as S=0.25 and for Richardson numbers (Ri=0.01, 1, 10 and 100).

The parameters kept constant are: the Reynolds number which is fixed at 100 and the solid volume fraction φ=0.04.

The variation of the mean Nusselt number of the heat source, with the nanofluid nature, at different Richardson numbers is depicted in the Tab. 7. The results show that with copper or silver nanoparticles, the mean Nusselt number is higher than with alumina or titanium nanoparticles, this is due to the highest values of their thermal conductivity in comparison with the other nanoparticles. The lowest mean Nusselt number is obtained for TiO_2 nanoparticles.

The Tab. 8 displays the percentage of heat transfer rate increase for the four types of nanofluids with respect to pure water, at several values of Richardson number. The highest increase in mean Nusselt number is obtained in the case of Cu-water nanofluid at Ri=0.01 and the lowest percentage increase is obtained for TiO_2-water nanofluid at Ri=10. The heat transfer increase is due to increase in effective thermal conductivity of the nanofluids, which results in better thermal transport of the fluid

Also, Fig. 12 illustrates the comparison between the average Nusselt number of copper-water nanofluid at φ=0.06 with average Nusselt number obtained for pure water with respect to Richardson number, the enhancement reaches 13.67% for Ri=0.01 (forced convection dominating regime).

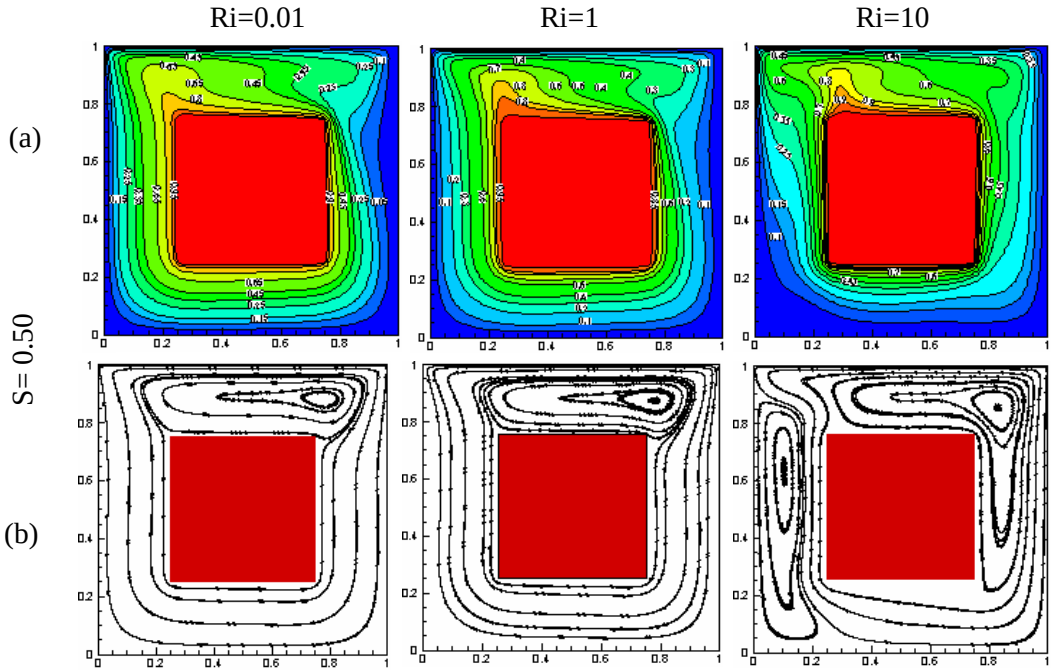

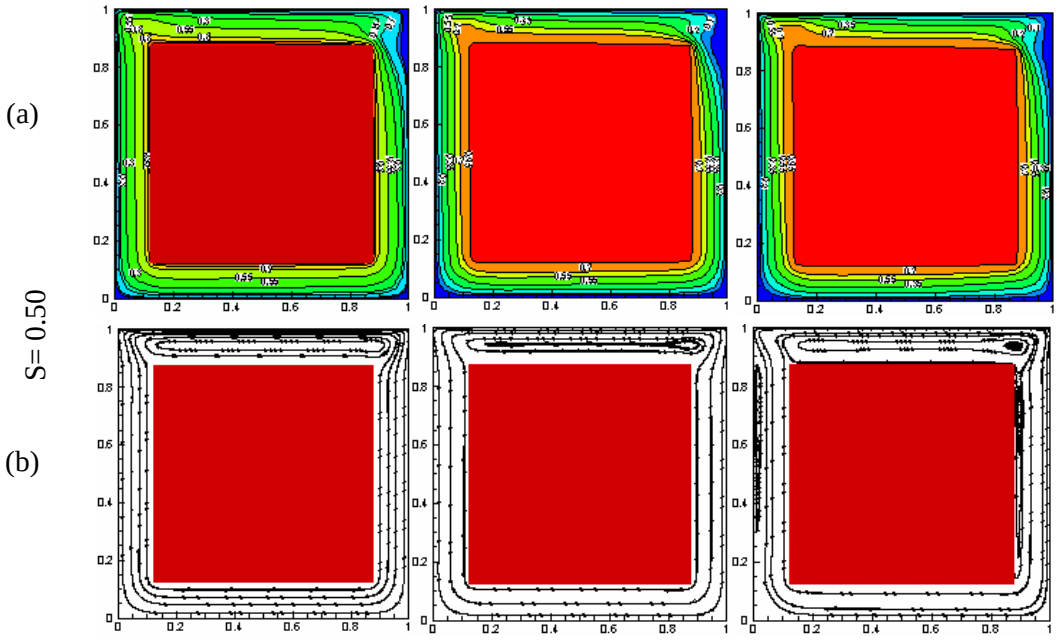

Figure 6: Isotherms (a) and streamlines (b) for copper-water filled cavity at different sizes of the heat source (S=0.5, 0.75), different Ri numbers, Re=100 and φ=0.04

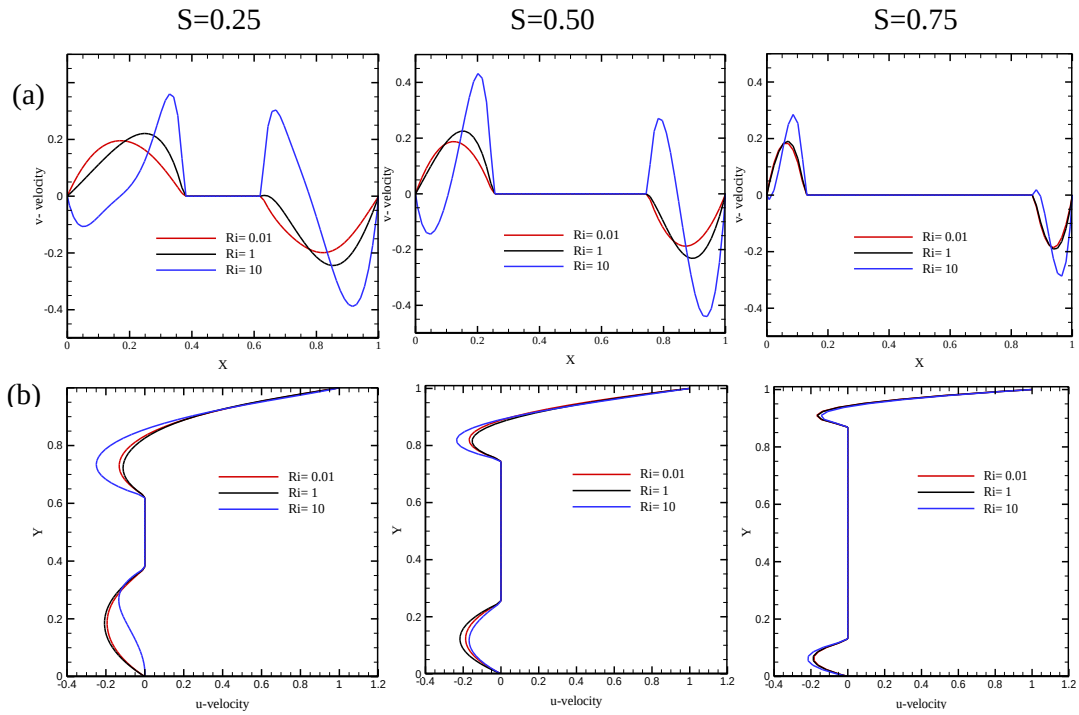

Figure 7: (a) v-velocity and (b) u-velocity profiles along the horizontal and vertical mid-planes in the copper-water filled cavity for different heat source sizes (S=0.25, 0.50, 0.75)

and at Richardson numbers (Ri=0.01, 1, 10), Re=100, φ=0.04

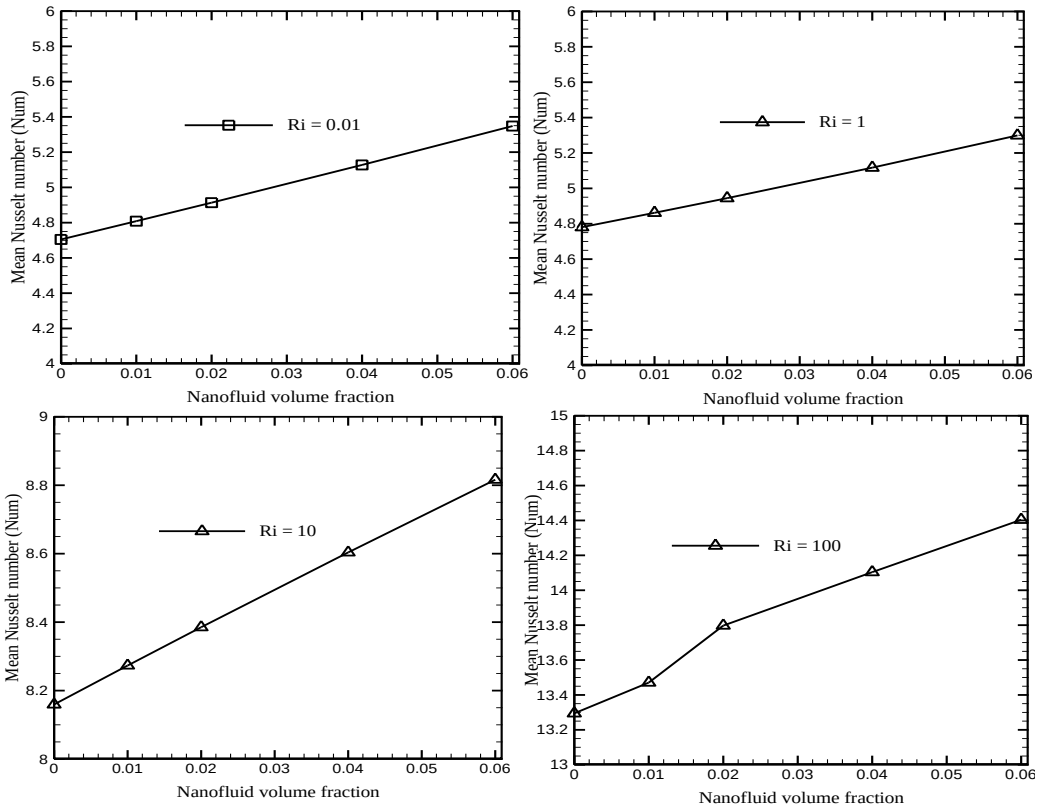

Figure 8: Effect of the nanoparticles volume fraction on the mean Nusselt number at different Richardson numbers (Ri=0.01, 1, 10, 100). The cavity is filled with copper-water nanofluid, Re=100 and S=0.25

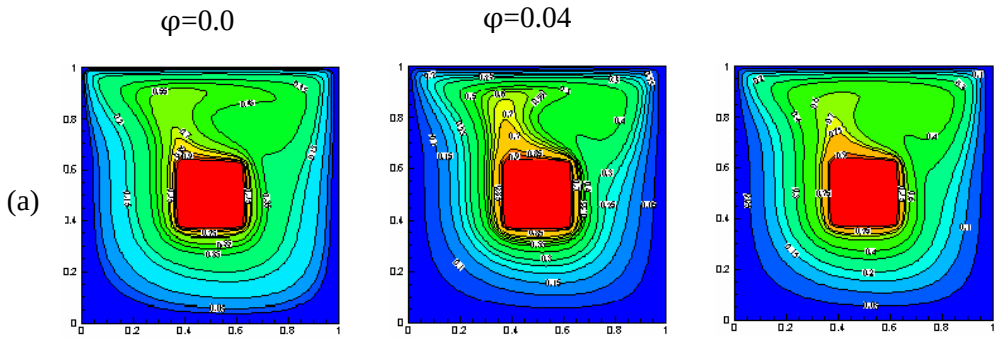

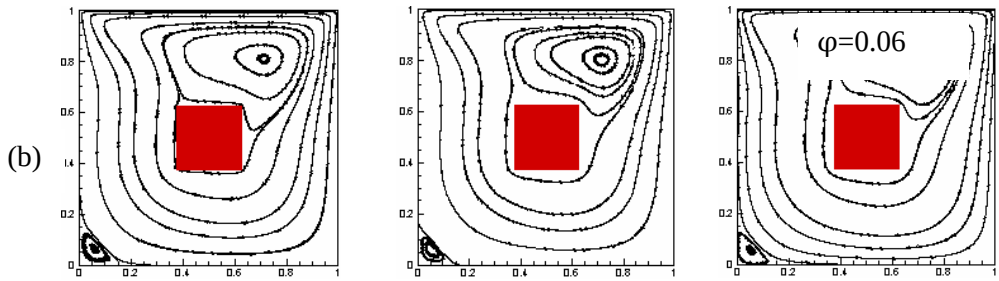

Figure 9: Isotherms (a) and streamlines (b) in the copper-water filled cavity at different solid volume fractions (φ=0, 0.04 and 0.06) for Ri=1, Re=100 and S=0.25

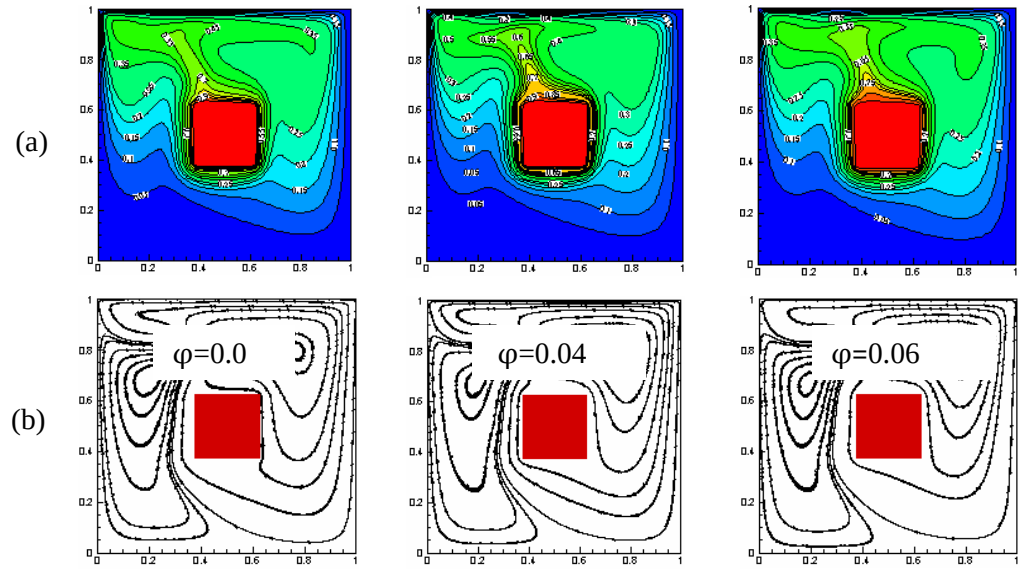

Figure 10: Isotherms (a) and streamlines (b) in the copper-water filled cavity at different solid volume fractions (φ=0, 0.04 and 0.06) for Ri=10, Re=100 and S=0.25

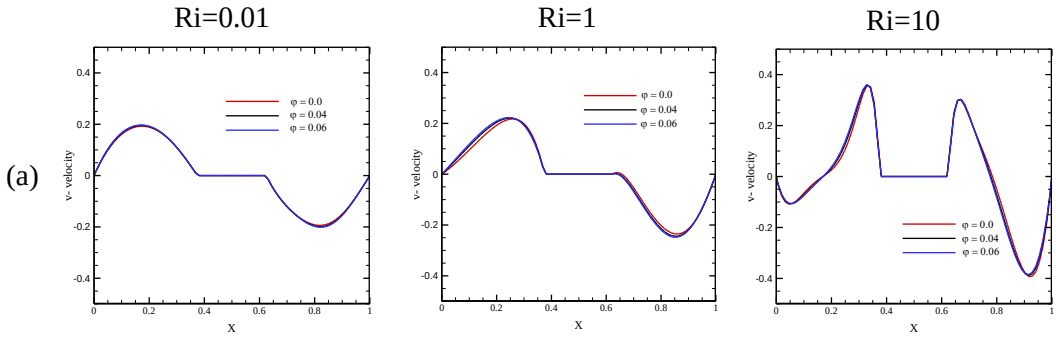

(b)

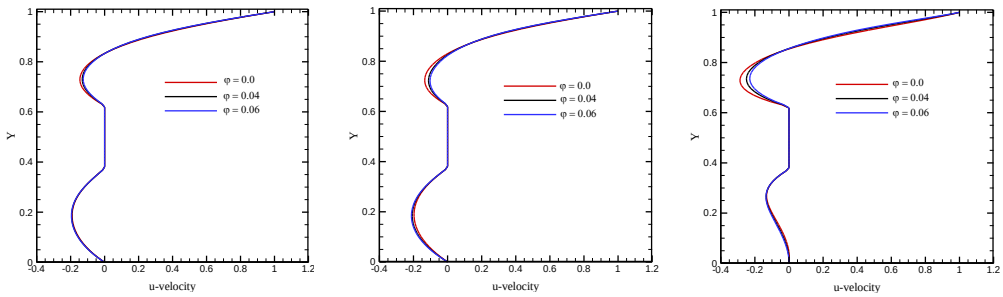

Figure 11: (a) v-velocity and u-velocity (b) profiles along the horizontal and vertical mid-planes in the copper-water filled cavity at various Richardson numbers (Ri=0.01, 1, 10) and for different solid volume fractions (φ=0.0, 0.04, 0.06) for Re=100 and S=0.25

Table 6: Variation of the maximum stream function with the nanofluid volume fraction at different Richardson numbers, Re=100 and S=0.25.

Maximum stream function ψ_{max}				
Ri/ φ	φ=0.00	φ=0.02	φ=0.04	φ=0.06
Ri=0.01	$2.6218e^{-6}$	$2.6909e^{-6}$	$2.7569e^{-6}$	$2.8176e^{-6}$
Ri=1	$3.8064e^{-5}$	$3.3655e^{-5}$	$2.9103e^{-5}$	$2.6278e^{-5}$
Ri=10	$1.4239e^{-2}$	$1.4037e^{-2}$	$1.4012e^{-2}$	$1.3954e^{-2}$

Table 7: Variation of the mean Nusselt number at the surface of the heat source with the nanofluid nature at different Richardson numbers, φ=0.04, Re=100 and S=0.25

Num					
Ri/ fluid	Num,w pure water	Cu-water	Ag-water	Al_2O_3-water	TiO_2-water
Ri=0.01	4.705	5.127	5.103	5.091	5.078
Ri=1	4.781	5.117	5.091	5.080	5.078
Ri=10	8.159	8.604	8.587	8.549	8.455
Ri=100	13.295	14.103	14.062	13.867	13.828

Table 8: Percentage of heat transfer rate increase for different nanofluids with respect to pure water at different Richardson numbers, φ=0.04, Re=100 and S=0.25.

((Num-Num, w)*100/Num, w) %				
Ri/ nanofluid type	Cu-water	Ag-water	Al_2O_3 water	TiO_2 water
Ri=0.01	8.969	8.459	8.204	7.928
Ri=1	7.028	6.484	6.254	6.212
Ri=10	5.454	5.246	4.780	3.628
Ri=100	6.077	5.769	4.302	4.009

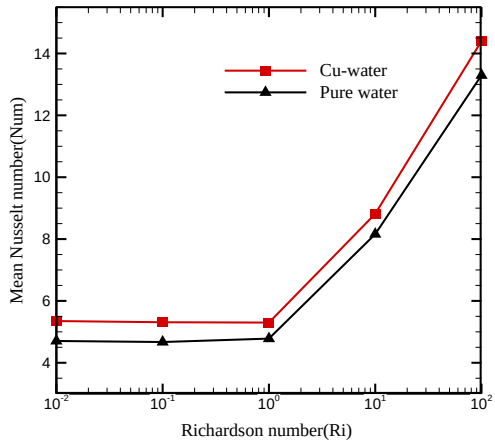

Figure 12: Comparison between the mean Nusselt number of the copper-water nanofluid at φ=0.06 with the mean Nusselt number obtained for pure water at different Richardson numbers (Ri=0.01, 0.1, 1, 10, 100), for Re=100 and S=0.25

5 Conclusion

This study has performed a numerical investigation into the mixed convection heat transfer performance of water-based nanofluids confined in a lid driven square enclosure with a centred isotherm heat source. In modelling the cavity, we assumed that all the walls are cooled at constant temperature Tc, and the top wall moves rightward at a constant velocity.

The governing equations were solved using finite volume approach by the SIMPLER algorithm. The simulations considered four types of nanofluids (Cu, Ag, Al_2O_3, TiO_2)-Water and focused on the effects of respectively the Richardson number, heat source size, solid volume fraction and nanofluid nature on the flow streamlines, isotherm distribution and mean Nusselt number. Following conclusions can be drawn from the numerical simulation results.

- For the following heat source size (S=0.25, 0.50), the mean Nusselt number remains constant with increasing the Richardson number until the latter reaches the value of 1, beyond which the mean Nusselt number increases more fastly. The results show that heat transfer is improved by 175.6% with increasing Ri from 1 to 100. For S=0.75, the mean Nusselt number doesn't change till the Richardson number reaches the value of Ri=10. For further increase in Richardson number, the mean Nusselt number increases rapidly. Increasing Ri leads to an intensification of the convective flow. As a result, we can produce a better cooling of the heat source by increasing the Richardson number to natural convection dominating regime. This will allow us to reduce the velocity of the lid and economize the energy required for its movement.
- We remark that for Ri≤10, the mean Nusselt number Num3 of the right face is better than the mean Nusselt of the other faces, but for Ri=100, the mean Nusselt number Num1 of the left face becomes higher than the other's
- We conclude that at a fixed Richardson number, the mean Nusselt number decreases when the heat source size is increased from S=0.25 to S=0.50, then increases for a further increase of the heat source size except in the case of Ri=100, where Num does not change when S increases from S=0.5 to S=0.75. The mean Nusselt number remains constant until Ri reaches Ri=10, in the case of S=0.75, but has higher values in comparison with the other heat source sizes. The highest mean Nusselt number is obtained for the lower size studied S=0.25 at Ri=100.
- Significant heat transfer enhancement could be obtained due to the inclusion of the nanoparticles into the base fluid. When the solid volume fraction of nanoparticles is increased, the mean Nusselt number increases and the temperature in the vicinity of the cavity is reduced for all the studied regimes. However, increasing the solid volume fraction of nanoparticles does not influence the intensity of the stream function for all the Richardson numbers studied.
- The comparison between the mean Nusselt number of copper-water nanofluid at φ=0.06 with mean Nusselt number obtained for pure water with respect to Richardson number shows that the enhancement reaches 13.67% for Ri=0.01 in forced convection dominating regime.
- Nanoparticles with higher thermal conductivity such as copper (Cu) and silver (Ag) produce a greater enhancement in the rate of heat transfer. Whereas, alumina (Al_2O_3) and oxide titanium (TiO_2) nanoparticles make lower performance.

References

Abu-Nada, E.; Chamkha, A. J. (2010): Mixed convection flow in a lid-driven inclined square enclosure filled with a nanofluid. *European Journal of Mechanics B/Fluids*, vol. 29, pp. 472-482.

Abdellahoum, C.; Mataoui, A.; Oztop, H. F. (2015): Turbulent forced convection of nanofluid over a heated shallow cavity in a duct. *Powder Technology*, vol. 277, pp. 126-134.

Abu-Nada E.; Oztop, H. (2011): Numerical analysis of Al_2O_3/water nanofluids in natural convection in a wavy walled cavity. *Numerical Heat Transfer, Part A*, vol. 59, pp. 403-419.

Chemloul, N. S.; Belmiloud, M. A. (2016): Effet des nanoparticules sur l'amélioration du transfert thermique dans une cavité carrée. *Revue des énergies renouvelables,* vol. 19, pp. 397-408.

Garoosi, F.; Bagheri, G.; Talebi, F. (2013): Numerical simulation of natural convection of nanofluids in a square cavity with several pairs of heaters and coolers (HACs) inside. *International Journal of Heat and Mass Transfer,* vol. 67, pp. 362-376.

Ghasemi, B.; Aminossadati, S. M. (2009): Natural convection heat transfer in an inclined enclosure filled with a water-cuo nanofluid. *International Journal of Computation and Methodology Numerical Heat Transfer, Part A,* vol. 55, pp. 807-823.

Heidary, H.; Kerman, M. J. (2012): Heat transfer enhancement in a channel with block(s) effect and utilizing Nanofluid. *International Journal of Thermal Sciences,* vol. 57, pp. 163-171.

Islam, A. W.; Sharif, M. A. R.; Carlson, E. S. (2012): Mixed convection in a lid driven square cavity with an isothermally heated square blockage inside. *International Journal of Heat and Mass Transfer,* vol. 55, pp. 5244-5255.

Kalteh, M.; Kourosh, J.; Toraj, A. (2014): Numerical solution of nanofluid mixed convection heat transfer in a lid-driven square cavity with a triangular heat source. *Powder Technology,* vol. 253, pp. 780-788.

Morshed, K. N.; Sharif, M. A. R.; Islam, A. W. (2015): Laminar mixed convection in a lid driven square cavity with two isothermally heated square internal blockages. *Chemical Engineering Communications*, vol. 202, pp. 1176-1190.

Moradi, H.; Bazooyar, B.; Moheb, A.; Etemad, S. G. (2015): Experimental study on natural convection heat transfer of Newtonian nanofluids in a cylindrical enclosure. *Chinese Journal of chemical engineering,* DOI 10.1016/J.CJCHE.2015.04.002.

Muthtamilselvan, M.; Kandaswamy, P.; Lee, J. (2010): Heat transfer enhancement of copper-water nanofluids in a lid-driven enclosure. *Communications in Nonlinear Science and Numerical Simulation,* vol. 15, pp. 1501-1510.

Moumni, H.; Welhezi, H.; Djebali, R.; Sediki, E. (2015): Accurate finite volume investigation of nanofluid mixed convection in two-sided lid driven cavity including discrete heat sources. *Applied Mathematical Modelling,* vol. 39, pp. 4164-4179.

Ögüt, E. B. (2009): Natural convection of water-based nanofluids in an inclined enclosure with a heat source. *International of Thermal Journal Sciences,* vol. 48, pp. 2063-2073.

Patankar, S. V. (1980): *Numerical heat transfer and fluid flow*. McGraw-Hill, NewYork.

Rahman, M. M.; Billah, M. M.; Hasanuzzaman, M.; Saidur, R.; Rahim, N. A. (2012): Heat transfer enhancement of nanofluids in a lid-driven square enclosure. *Numerical Heat Transfer, Part A,* vol. 62, pp. 973.

Rashmi, W.; Khalid, M.; Ismail, A. F.; Saidur, R.; Rashid, A. K. (2015): Experimental and numerical investigation of heat transfer in CNT nanofluids. *Journal of Experimental Nanoscience,* vol. 10, pp. 545-563.

Rashidi, I.; Mahian, O.; Lorenzini, G.; Biserni, C.; Wongwises, S. (2014): Natural convection of Al_2O_3/water nanofluid in a square cavity: Effects of heterogeneous heating.

International Journal of Heat and Mass Transfer, vol. 74, pp. 391-402.

Roslan, R. H.; Saleh, H.; Hashim, I. (2012): Effect of rotating cylinder on heat transfer in a square enclosure filled with nanofluids. *International Journal of Heat and Mass Transfer*, vol. 55 pp. 7247-7256.

Rahman, M. M.; Parvin, S.; Rahim, N. A; Islam, M. R.; Saidur, R.; Hasanuzzaman, M. (2012): Effects of Reynolds and Prandtl number on mixed convection in a ventilated cavity with a heat-generating solid circular block. *Applied Mathematical Modelling*, vol. 36, pp. 2056-2066.

Selimefendigil, F.; Oztop, H. (2014): Numerical study of MHD mixed convection in a nanofluid filled lid driven square enclosure with a rotating cylinder. *International Journal of Heat and Mass Transfer*, vol. 78, pp. 741-754.

Sivasankaran, S.; Pan, K. L. (2014): Natural convection of nanofluids in a cavity with nonuniform temperature distributions on side walls. *Numerical Heat Transfer, Part A*, vol. 65, pp. 247-268

Wang, G.; Meng, X.; Zeng, M.; Ozoe, H. C.; Wang, Q. W. (2014): Natural convection heat transfer of copper-water nanofluid in a square cavity with time-periodic boundary temperature. *Heat Transfer Engineering*, vol. 35, pp. 630-640.